

Supporting Information

Non-traditional thermal behavior of Co(II) coordination networks showing slow magnetic relaxation

Anna Świtlicka^{a*}, Barbara Machura^a, Alina Bieńko^{b*}, Sandra Kozieł^b, Dariusz C. Bieńko^c, Cyril Rajnák^d, Roman Boča^d, Andrew Ozarowski^e and Mykhaylo Ozerov^e

^a Department of Crystallography, Institute of Chemistry, University of Silesia, 9th Szkolna St., 40-006 Katowice, Poland, E-mail: anna.switlicka@us.edu.pl

^b Faculty of Chemistry, University of Wroclaw, 14 F. Joliot-Curie, 50-383 Wroclaw, Poland, E-mail: alina.bienko@chem.uni.wroc.pl

^c Faculty of Chemistry, Wroclaw University of Technology, Wybrzeze Wyspiańskiego 27, 50-370 Wroclaw, Poland

^d Department of Chemistry, Faculty of Natural Sciences, University of SS Cyril and Methodius, 91701 Trnava, Slovakia

^e National High Magnetic Field Laboratory, Florida State University, 1800 East Paul Dirac Drive, Tallahassee, Florida 32310, United States

Compounds under study

1, [Co(5,6-(Me)₂-bzim)₂(dca)₂]_n, C₂₂H₂₀N₁₀Co ($M = 483.41 \text{ g mol}^{-1}$), CCDC 2085569

2, [Co(5-Mebzim)₂(dca)₂]_n, C₂₀H₂₂N₁₀Co ($M = 461.40 \text{ g mol}^{-1}$), CCDC 2085570

3, [Co(2-Mebzim)(dca)₂]_n, C₂₀H₁₆N₁₀Co ($M = 455.36 \text{ g mol}^{-1}$), CCDC 2085571

Supporting Information.....	1
1. Synthesis and characterization.....	3
Figure S1. The powder XPRD pattern of 1	4
Figure S2. The powder XPRD pattern of 2	4
Figure S3. The powder XPRD pattern of 3	4
Figure S7. UV/Vis spectra of 1–3	6
Table S1. Electronic spectral data for 1–3	6
2. X-Ray structure data	7
Table S2. Bond lengths [Å] and angles [°] in 1	7
Table S3. Bond lengths [Å] and angles [°] in 2	7
Table S4. Bond lengths [Å] and angles [°] in 3	8
Table S5. Short intra- and intermolecular contacts in the structures.	8
Table S6. Magneto-structural relationships in 1D cobalt(II)-dicyanamido complexes	9
Table S7. Magneto-structural relationships of 2D cobalt(II)-dicyanamido complexes.....	14
3. The HFEPR and FIRMS spectra	21
Figure S8. Blue traces: HF EPR spectra of compounds 1 and 2 recorded at similar conditions.....	21
Figure S9. Blue traces: HF EPR spectra of compounds 3	21
4. Selected AC susceptibility data	22
Figure S10. Field dependence of the AC susceptibility for 1 through 3 at $T = 2.0$ K for a set of trial frequencies. Lines – guide for eyes.	22
Figure S11. Temperature dependence of the AC susceptibility for 1 through 3 at $B_{DC} = 0.2$ T for 22 frequencies of the oscillating field.	23
Figure S12. Frequency dependence of the AC susceptibility at $B_{DC} = 0.2$ T. Lines – fitted, using the two-set Debye model.	24
Figure S13. Argand plot (left) and the Arrhenius-like plot (right). Solid line – fitted with Raman-like and phonon-bottleneck terms $\tau^{-1} = CT^n + FT^l$	25
Figure S14. Various dependences of the high-frequency relaxation time. Dashed (dot-dashed) lines – linear fits to the high-temperature (low-temperature) windows. Solid – combined Raman-like and phonon-bottleneck terms.	26

1. Synthesis and characterization

Materials. The reagents used to the synthesis were commercially available and they were used without further purification.

Preparation of the complexes. $\text{NaN}(\text{CN})_2$ (0.075 g, 0.84 mmol) dissolved in water (5 cm³) was added to a deep pink methanolic solution of $\text{CoCl}_2 \cdot 6\text{H}_2\text{O}$ (0.10 g, 0.42 mmol) and suitable benzimidazole derivatives (0.84 mmol). The resulting mixture was filtered and allowed to evaporate at room temperature. X-ray quality pink crystals of **1–3** were grown after few days and they were collected by filtration and air-dried.

[Co(5,6-(Me)₂-bzim)₂(dca)₂]_n (1): Yield 80%. IR (KBr, cm⁻¹): 3203(m) $\nu(\text{N}-\text{H})$; 2274(s) ν_{as} + $\nu_s(\text{C}\equiv\text{N}_{\text{dca}})$; 2253(s) $\nu_{\text{as}}(\text{C}\equiv\text{N}_{\text{dca}})$; 2187(vs) $\nu_s(\text{C}\equiv\text{N}_{\text{dca}})$; 1507(m), 1399(m) and 1312(s) $\nu(\text{C}=\text{N})$ and $\nu(\text{C}=\text{C})$. Anal. calcd for $\text{C}_{22}\text{H}_{20}\text{N}_{10}\text{Co}$ (483.41 g/mol) C, 54.66; H, 4.17; N, 28.98; found C, 54.28, H, 4.04; N, 28.81%.

[Co(5-Mebzim)₂(dca)₂]_n (2) Yield 75%. IR (KBr, cm⁻¹): 3227(m) $\nu(\text{N}-\text{H})$; 2276(s) ν_{as} + $\nu_s(\text{C}\equiv\text{N}_{\text{dca}})$; 2251(s) $\nu_{\text{as}}(\text{C}\equiv\text{N}_{\text{dca}})$; 2185(vs) $\nu_s(\text{C}\equiv\text{N}_{\text{dca}})$; 1503(m), 1408(m) and 1318(s) $\nu(\text{C}=\text{N})$ and $\nu(\text{C}=\text{C})$. Anal. calcd for $\text{C}_{20}\text{H}_{22}\text{N}_{10}\text{Co}$ (461.40 g/mol) C, 52.06; H, 4.81; N, 30.36 found C, 52.16; H, 4.52; N, 30.76%.

[Co(2-Mebzim)(dca)₂]_n (3) Yield 75%. IR (KBr, cm⁻¹): 3368(m) $\nu(\text{N}-\text{H})$; 2277(s) ν_{as} + $\nu_s(\text{C}\equiv\text{N}_{\text{dca}})$; 2248(s) $\nu_{\text{as}}(\text{C}\equiv\text{N}_{\text{dca}})$; 2177(vs) $\nu_s(\text{C}\equiv\text{N}_{\text{dca}})$; 1534(m), 1456(s) and 1322(s) $\nu(\text{C}=\text{N})$ and $\nu(\text{C}=\text{C})$. Anal. calcd for $\text{C}_{20}\text{H}_{16}\text{N}_{10}\text{Co}$ (455.36 g/mol) C, 52.76; H, 3.54; N, 30.76 found C, 52.55; H, 3.47; N, 30.80%.

Physical techniques. The UV-Vis spectra were recorded from solid state samples on Nicolet Evolution 220 and spectrophotometer Nicolet iS50 FT-IR in the ranges 190–1100 nm and 700–1500 nm, respectively (see ESI). IR spectra were recorded on a Nicolet iS5 spectrophotometer in the spectral range 4000–400cm⁻¹ with the samples as of KBr pellets. Elemental analysis was registered by Vario EL III apparatus (Elementar, Germany).

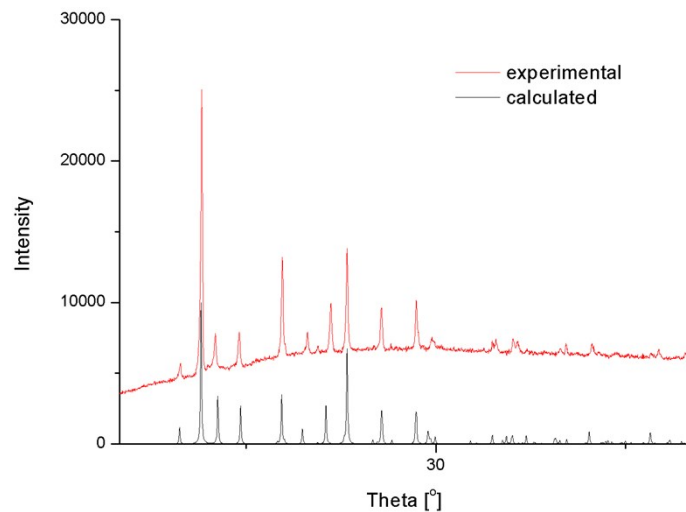


Figure S1. The powder XPRD pattern of **1**.

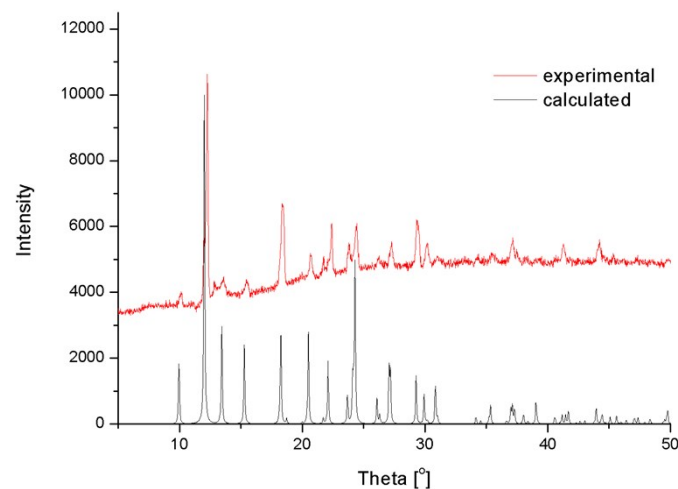


Figure S2. The powder XPRD pattern of **2**.

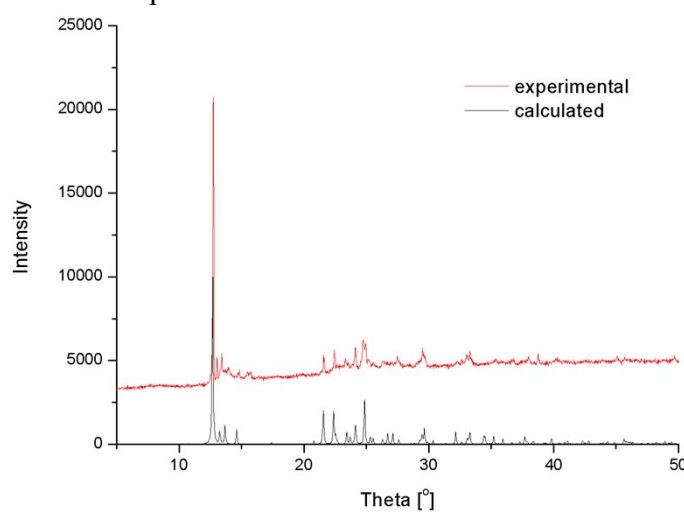


Figure S3. The powder XPRD pattern of **3**.

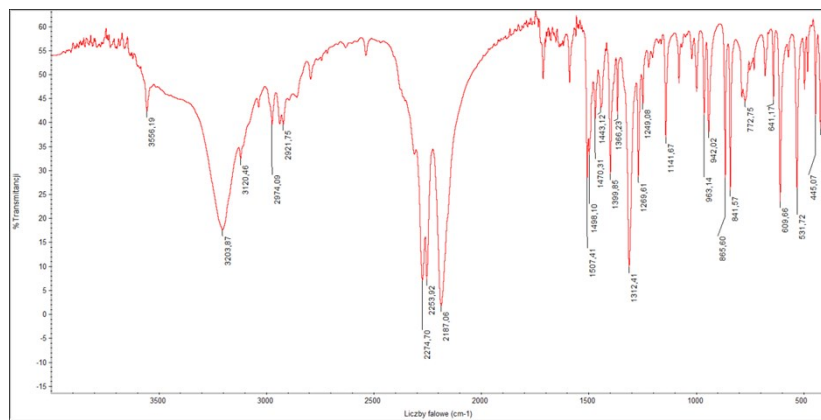


Figure S4. IR spectrum of **1**.

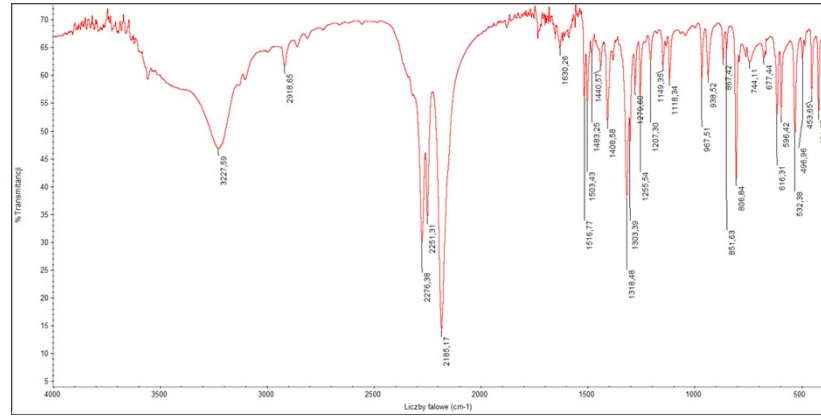


Figure S5. IR spectrum of **2**.

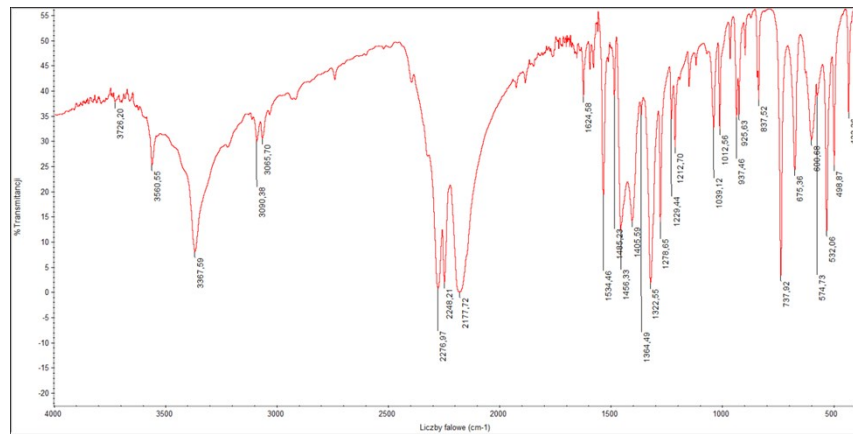


Figure S6. IR spectrum of **3**.

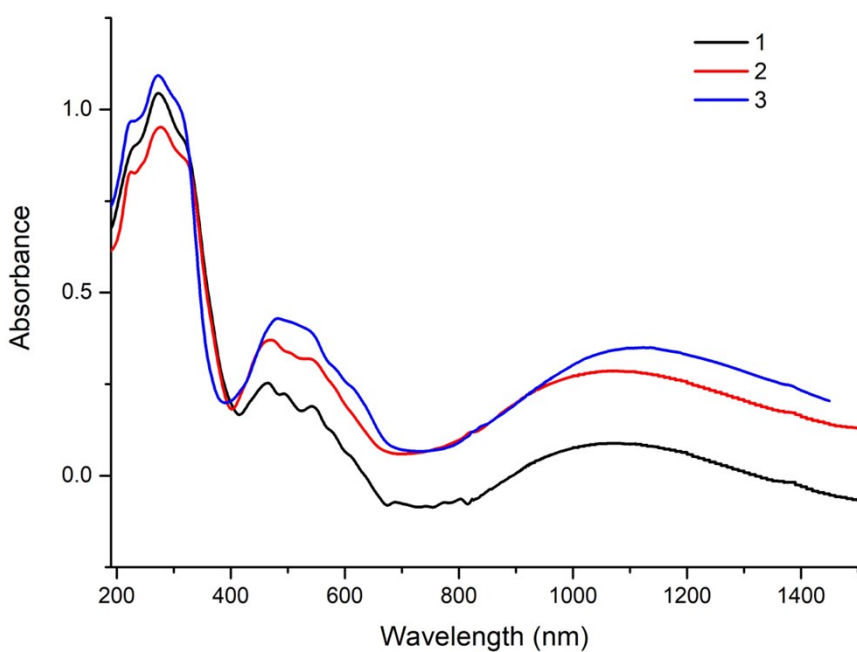


Figure S7. UV/Vis spectra of **1–3**.

Table S1. Electronic spectral data for **1–3**

Compound	$\lambda_{max}/\text{nm}(\text{cm}^{-1})$	Dq/cm^{-1} ^a	B/cm^{-1} ^b
1	1064 (9398), 546 (18315), 494 (20242), 465 (21505), 314 (31847), 275 (36363), 228 (43859)	892	691
2	1056 (9469), 545 (18348), 499 (20040), 465 (21505), 322 (31055), 279 (35842), 226 (44247)	888	665
3	1079 (9267), 543 (18416), 481 (20790), 307 (32573), 272 (36764), 225 (44445)	915	760

^a $10Dq$ – ligand field splitting parameter

^b B – Racah parameter of the interelectrone repulsion.

2. X-Ray structure data

Table S2. Bond lengths [\AA] and angles [$^\circ$] in 1

Bond lengths		Bond angles	
Co(1)–N(1)	2.1165(19)	N(1)–Co(1)–N(1)a	180.0
Co(1)–N(1)a	2.1165(19)	N(1)–Co(1)–N(99)a	88.75(5)
Co(1)–N(99)	2.1981(14)	N(1)a–Co(1)–N(99)a	91.25(5)
Co(1)–N(99)a	2.1981(14)	N(1)–Co(1)–N(99)b	91.25(5)
Co(1)–N(99)b	2.1981(14)	N(1)a–Co(1)–N(99)b	88.75(5)
Co(1)–N(99)c	2.1981(14)	N(99)a–Co(1)–N(99)b	86.14(7)
		N(1)–Co(1)–N(99)c	88.75(5)
		N(1)a–Co(1)–N(99)c	91.25(5)
		N(99)a–Co(1)–N(99)c	93.86(7)
		N(99)b–Co(1)–N(99)c	180.00(5)
		N(1)–Co(1)–N(99)	91.25(5)
		N(1)a–Co(1)–N(99)	88.75(5)
		N(99)a–Co(1)–N(99)	180.0
		N(99)b–Co(1)–N(99)	93.86(7)
		N(99)c–Co(1)–N(99)	86.14(7)
		C(99)–N(99)–Co(1)	161.49(12)
		C(99)–N(98)–C(99)b	120.20(18)
		N(99)–C(99)–N(98)	175.43(15)
		N(99)–C(99)–N(98)	175.1(2)

Symmetry codes: (a): $1-x, y, 1-z$; (b): $1-x, 1-y, 1-z$; (c): $x, 1-y, z$

Table S3. Bond lengths [\AA] and angles [$^\circ$] in 2

Bond lengths		Bond angles	
Co(1)–N(1)	2.122(3)	N(1)–Co(1)–N(1)d	180.0
Co(1)–N(1)d	2.122(3)	N(1)–Co(1)–N(99)e	90.30(7)
Co(1)–N(99)	2.141(2)	N(1)d–Co(1)–N(99)d	90.30(7)
Co(1)–N(99)d	2.141(2)	N(1)–Co(1)–N(99)d	89.70(7)
Co(1)–N(99)e	2.141(2)	N(1)d–Co(1)–N(99)e	89.70(7)
Co(1)–N(99)f	2.141(2)	N(99)d–Co(1)–N(99)e	89.69(11)
		N(1)–Co(1)–N(99)f	89.70(7)
		N(1)d–Co(1)–N(99)f	90.30(7)
		N(99)d–Co(1)–N(99)f	90.31(11)
		N(99)e–Co(1)–N(99)f	180.00(11)
		N(1)–Co(1)–N(99)	90.30(7)
		N(1)d–Co(1)–N(99)	89.70(7)
		N(99)d–Co(1)–N(99)	180.0
		N(99)e–Co(1)–N(99)	90.31(11)
		N(99)f–Co(1)–N(99)	89.69(11)
		C(99)–N(99)–Co(1)	160.41(19)
		C(99)e–N(98)–C(99)	117.8(3)

Symmetry codes: (d): $-x, y, -z$; (e): $-x, -y, -z$; (f): $x, -y, z$

Table S4. Bond lengths [\AA] and angles [$^\circ$] in **3**

Bond lengths		Bond angles	
Co(1)–N(1)	2.1513(18)	N(1)–Co(1)–N(1) ^g	180.0
Co(1)–N(1) ^g	2.1513(18)	N(1)–Co(1)–N(97)	92.63(7)
Co(1)–N(97)	2.1445(19)	N(1)–Co(1)–N(97) ^g	87.37(7)
Co(1)–N(97) ^g	2.1445(19)	N(1)–Co(1)–N(99)	93.25(7)
Co(1)–N(99)	2.1405(19)	N(1)–Co(1)–N(99) ^g	86.75(7)
Co(1)–N(99)	2.1405(19)	N(1) ^g –Co(1)–N(99)	86.75(7)
		N(1) ^g –Co(1)–N(99) ^g	93.25(7)
		N(1) ^g –Co(1)–N(97)	87.37(7)
		N(1) ^g –Co(1)–N(97) ^g	92.63(7)
		N(99)–Co(1)–N(97)	93.98(7)
		N(99) ^g –Co(1)–N(97)	86.02(7)
		N(99)–Co(1)–N(97) ^g	86.02(7)
		N(99) ^g –Co(1)–N(97) ^g	93.98(7)
		N(99)–Co(1)–N(99) ^g	180.0
		N(97)–Co(1)–N(97) ^g	180.0
		C(98)–N(97)–Co(1)	151.16(18)
		C(99)–N(99)–Co(1)	160.73(19)
		N(99)–C(99)–N(98)	173.2(2)
		N(97)–C(98)–N(98) ^g	173.4(2)
		C(98) ^g –N(98)–C(99)	119.7(2)

Symmetry codes: (g): $1-x, -y, 1-z$ **Table S5.** Short intra- and intermolecular contacts in the structures.

D—H \cdots A	D—H	H \cdots A	D \cdots A [\AA]	D—H \cdots A [$^\circ$]
1				
N(2)–H(2) \cdots N(99) ^h	0.86	2.13	2.979(3)	169.0
2				
N(2)–H(2) \cdots N(98) ⁱ	0.86	2.16	2.983(5)	159.0
3				
N(2)–H(2) \cdots N(98) ^j	0.86	2.34	3.104(3)	149.0

Symmetry elements: (h): $-1/2+x, 1/2+y, z$; (i): $1/2-x, -1/2+y, -z$; (j): $1/2+x, 1/2-y, -1/2+z$

Table S6. Magneto-structural relationships in 1D cobalt(II)-dicyanamido complexes

Compound /	Co–N _L /Co–O	Co–N _{dca}	Co…Co	Magnetic properties	Ref.
single μ-1,5-dca bridge					
[Co(L ¹) ₄ (dca)] _n (ClO ₄) _n ·4n(EtOH)·nH ₂ O	2.121(4) 2.121(4)	2.088(8) 2.063(9)	8.6090(5)	C = 3.32 cm ³ mol ⁻¹ K Θ = -31.8 K weak AF interaction	1
[Co(hypy) ₂ (dca)(MeOH) ₂] _n	2.138(3) 2.138(3) Co–O= 2.123(3) Co–O= 2.123(3)	2.103(4) 2.103(4)	8.665	C = 3.123 cm ³ mol ⁻¹ K, Θ = -16.29 K.	13
[Co(biim) ₂ (dca) ₂]Cl	2.1386(18) 2.1593(18) 2.1372(18) 2.1325(18)	2.1133(19) 2.1900(19)	7.286	D = 40.3 cm ⁻¹ , J/kB = 20.05 cm ⁻¹	17
[Co(enbzpy)(dca)] _n (ClO ₄) _n	room temperature 2.102(3) 2.083(3) 2.023(3) 2.028(3) low temperature 2.138(8) 2.074(8) 2.089(8) 2.133(8)	room temperature 2.092(3) 2.136(3) low temperature 2.141(9) 2.073(8)	8.57	SCO	18
[Co(enbzpy)(dca)] _n (PF ₆) _n	room temperature 2.109(5) 2.045(4) 2.034(9) 2.097(4) Low temperature 2.039(6) 1.921(6)	room temperature 2.127(5) 2.134(5) Low temperature 2.163(7)	room temperature 8.699 Å low temperature 8.718	SCO	20

	1.916(6) 2.043(7)	2.181(8)			
[Co(bpym)(dca) ₂]·H ₂ O	2.151(3) 2.151(3) Co—O _{H2O} =2.124(4)	2.092(4) 2.103(5)	8.649	J= -1.42 Θ= -5.4 K	21
[Co(L ⁵)(dca)] _n	1.985 (4) 1.951 (3) Co-O=1.965 (3)	1.956 (4) 2.330 (5)	5.949	J = -3.52 cm ⁻¹	4
[Co(L ⁹)(dca) ₂] _n	2.086(2) 2.240(2) 2.154(2) 2.042(3)	2.164(2) 2.098(2)	8.542	C = 2.8–3.4 cm ³ mol ⁻¹ K J = -0.21 K	9
[Co(tpz)(dca)(H ₂ O)](dca)	2.213(2) 2.078(2) 2.221(2) Co- O _{H2O} = 2.005(2)	2.104(2) 2.096(2)	8,465	θ=7.97 K C=2.59 cm ³ Kmol ⁻¹	22
[Co(L ⁷)(dca)(ClO ₄) ₂ MeOH] _n	Co(A) 2.1619(19) 2.0785(19) 2.1011(18) 2.1323(19) Co(B) 2.141(2) 2.1017(19) 2.097(2) 2.1661(19)	Co(A) 2.1828(18) 2.0851(19) Co(B) 2.1013(18) 2.089(2)	8.451 Å 8.532 Å	lack of significant magnetic interactions	6
double μ-1,5-dca bridge					
[Co(im) ₂ (dca) ₂] _n	2.095(2) 2.095(2)	2.157(2) 2.157(2) 2.153(2) 2.153(2)	7.359	C = 2.8–3.4 cm ³ mol ⁻¹ J = -24.8 K	5
[Co(im) ₂ (dca) ₂] _n	2.101(2)	2.161(2)	7.395(1)	C = 2.8–3.4 cm ³ K mol ⁻¹	11

	2.101(2)	2.161(2) 2.164(3) 2.164(3)		J = -1.0 K	
[Co(ampy) ₂ (dca) ₂]	2.193(3) 2.193(3)	2.126(2) 2.126(2) 2.128(2) 2.128(2)		-	2
[Co(4omp) ₂ (dca) ₂] _n	2.126(4) 2.126(4)	2.116(4) 2.116(4) 2.124(5) 2.124(5)	7.076(3)	C = 3.58 cm ³ mol ⁻¹ $\Theta = -15.5$ K	14
[Co(pyr) ₂ (dca) ₂] _n	Co-O= 2.097(2) Co-O = 2.072(3)	2.084 (3) 2.084 (3) 2.099 (2) 2.099 (2)	7.220	weak antiferromagnetic interaction	15
[Co(mepy) ₂ (dca) ₂] _n	2.1229 (18) 2.1229 (18)	2.1385 (17) 2.1385 (17) 2.1385 (17) 2.1385 (17)	7.305(1)		24
[Co(4-nic) ₂ (dca) ₂] _n ·2nCH ₃ OH	2.157(2) 2.157(2)	2.114(3) 2.114(3) 2.128(2) 2.128(2)	7.353	C = 3.58 cm ³ ·mol ⁻¹ ·K, $\theta = -17.8$ K	26
[Co(dca) ₂ (H ₂ O) ₂] _n ·(hmt) _n	Co- O _{H2O} = 2.082(1)	2.122(2) 2.118(2)	7.362	J = -0.50 cm ⁻¹	3
(Ph ₄ P)[Co(dca) ₄]	-	2.176(3) 2.091(3) 2.165(3) 2.176(3) 2.091(3) 2.165(3)	7.589(1)	C= 1.394 cm ³ mol ⁻¹ $\Theta= +0.1$ K very weak ferromagnetic interaction	7

[Co(phen)(dca) ₂ (H ₂ O)·MeOH] _n	2.210(2) 2.210(2) 2.126(2) 2.112(2) Co-O _{H2O} = 2.127(2)	2.106(2) 2.102(2)	7.3244(5)	-	8
[Co(bipy)(dca) ₂] _n	2.129(2) 2.129(2)	2.134(2) 2.134(2) 2.102(2) 2.102(2)	7.375(1)	D= 93.7cm ⁻¹	12
[Co(mepypz) ₂ (dca) ₂] _n	Co-O= 2.109(2) Co-O= 2.109(2)	2.122(3) 2.122(3) 2.102(3) 2.102(3)	7.379(3)	-	16
[Co(pydz) ₂ (dca) ₂] _n	2.166(2) 2.166(2)	2.1095(14) 2.1095(14) 2.1095(14) 2.1095(14)	7.3409(5)	weak AF interaction <i>C</i> =3.46 cm ³ K mol ⁻¹ Θ = -20.46	19
[Co(L ²¹) ₂ (dca) ₂] _n	2.154(3) 2.154(3)	2.130(3) 2.130(3) 2.122(3) 2.122(3)	7.481(1)	-	23
{[Co(bpm) ₂ (dca)](ClO ₄) _n	2.141(4) 2.141(4)	2.103(5) 2.103(5) 2.103(5) 2.103(5)	7.592	-	25
double μ-1,5-dca bridge and N-donor ligand					
[Co(bpds)(dca) ₂] _n	2.180(5) 2.180(5)	2.143(5) 2.142(5) 2.143(5) 2.142(5)	7.302	J = -0.95 cm ⁻¹	3
[Co ₂ (tppz)(dca) ₄] _n	2.156(2) 2.156(2)	2.044(2) 2.044(2)	7.377 A	J = -1.10 cm ⁻¹	10

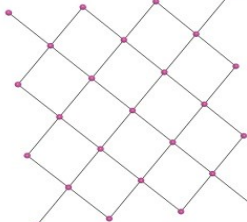
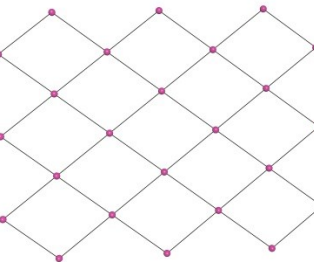
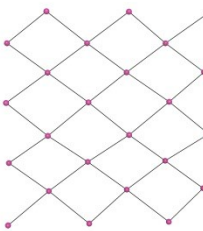
	2.114(2) 2.114(2) 2.140(2) 2.140(2)	2.141(2) 2.141(2)			
--	--	----------------------	--	--	--

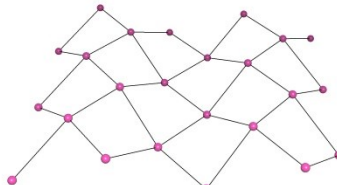
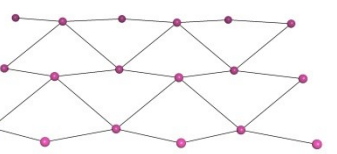
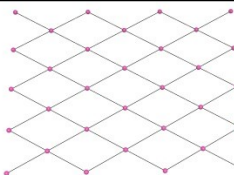
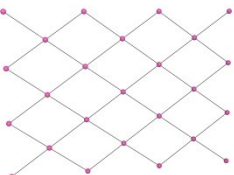
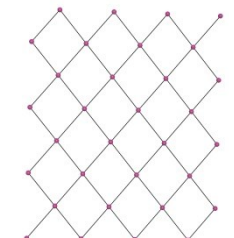
L¹= 4-(imidazol-1-yl)phenol; **L²**= anion N-(picolinoyl)biurate; **L³**= (N,N-diethyl,N'-(pyridin-2-yl)benzylidene)ethane-1,2-diamine; **L⁴** = N⁴-Schiff base ligand; **ampy**= 2-aminopyridine; **hmt**= hexamethylenetetramine; **bpds**= 4,4'-bipyridyl disulfide; **im**=imidazole; **phen**=4,7-phenanthroline; **tppz**= tetra-2-pyridylpyrazine; **bipy**= 4,4'-bipyridine; **hypy**= 3-hydroxypyridine; **pyr**=2-pyrrolidone; **mepypz**= 3,5-dimethyl-1-(2-pyridyl)pyrazole; **biim**= 2,2'-biimidazole; **enbzpy**= N,N'-bis(2-pyridinylbenzylidene)ethane-1,2-diamine; **pydz** = pyridazine, **bpym**= bipyrimidine; **tpz**= 2,4,6-tri(2-pyridyl)-1,3,5-triazine; **L⁵**= 4-picolylium chloride); **mepy**= 4-methylpyridine; **bpm**= bis(3,5-dimethyl)pyrazolylmethane; **4omp** = 4-methoxypyridine; **4-nic**= isonicotinamide

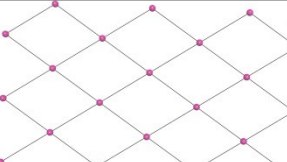
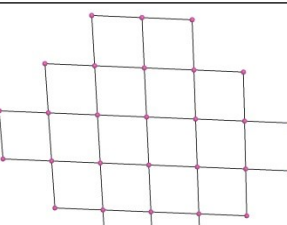
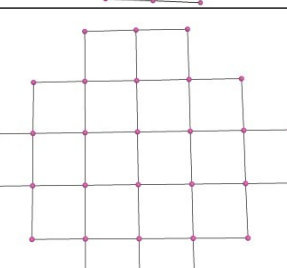
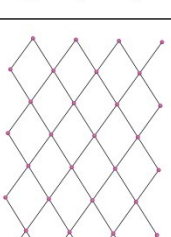
1. L. Zheng, S. Hu, A. Zhou, *Trans. Met. Chem.*, 2015, 40, 637–642.
2. A. C. B. Yuoh, M. Ondoh Agwara, D. Mbom Yufanyi, M. Aseng Conde, R. Jagan, K. Oben Eyong, *Internat. J. Inorg. Chem.*, 2015, 1–8.
3. S. C. Manna, A. Kumar Ghosh, J. Ribas, M. G.B. Drew, C.-N. Lin, E. Zangrandi, N. Ray Chaudhuri, *Inorg. Chim. Acta*, 2006, 359, 1395–1403.
4. M. Biswas, G. Pilet, M. S. El Fallah, J. Ribas, S. Mitra, *Inorg. Chim. Acta*, 2008, 361, 387–392.
5. R. Sen, A. Bhattacharjee, P. Gütlich, Y. Miyashita, K.-I. Okamoto, S. Koner, *Inorg. Chim. Acta*, 2009, 362, 4663–4670.
6. S. Banerjee, S. Halder, P. Brandão, C. J. Gómez García, S. Benmansour, A. Saha, *Inorg. Chim. Acta*, 2017, 464, 65–73.
7. L. Jäger, C. Wagner, M. Korabik, A. Zygmunt, J. Mroziński, *J. Mol. Struct.*, 2001, 570, 159–164.
8. D. S. Tonzing, S. R. Batten, K. S. Murray, *J. Mol. Struct.*, 2006, 796, 63–68.
9. S. Kundu, S. Roy, K. Bhar, R. Ghosh, C.-H. Lin, J. Ribas, B. Kumar Ghosh, *J. Mol. Struct.*, 2013, 1038, 78–85.
10. G.-Y. Hsu, C.-W. Chen, S.C. Cheng, S.-H. Lin, H.-H. Wei, C.-J. Lee, *Polyhedron*, 2005, 24, 487–494.
11. A. Das, C. Marschner, J. Cano, J. Baumgartner, J. Ribas, M. Salah El Fallah, S. Mitra, *Polyhedron*, 2009, 28, 2436–2442.
12. L. Vahovska, I. Potočnák, S. Vitushkina, M. Dušek, J. Titiš, R. Boča, *Polyhedron*, 2014, 81, 396–408.
13. L. Ling Zheng, C. Xia Zhou, S. Hu, A. J. Zhou, *Polyhedron*, 2016, 104, 91–98.
14. F. A. Mautner, M. Traber, R. C. Fischer, S. S. Massoud, R. Vicente, *Polyhedron*, 2017, 138, 13–20.
15. B.-Wa. Sun, So. Gao, B.-Q. Ma, Z.-M. Wang, *Inorg. Chem. Commun.*, 2001, 4, 72–75.
16. P. Pal, S. Konar, P. Lama, K. Das, A. Bauza, A. Frontera, S. Mukhopadhyay, *J. Phys. Chem. B*, 2016, 120, 6803–6811.
17. S. R. Marshall, C. D. Incarvito, W. W. Shum, A. L. Rheingold, J.S. Miller, *Chem. Commun.*, 2002, 3006–3007.
18. K. Bhar, S. Khan, J. Sanchez Costa, J. Ribas, O. Roubeau, P. Mitra, B. Kumar Ghosh, *Angew. Chem. Int. Ed.*, 2012, 51, 2142–2145.
19. M. Wriedt, C. Näther, *Dalton Trans.*, 2011, 40, 886–898.
20. S. Roy, S. Choubey, K. Bhar, N. Sikdar, J. Sánchez Costa, P. Mitra, B. Kumar Ghosh, *Dalton Trans.*, 2015, 44, 7774–7776.

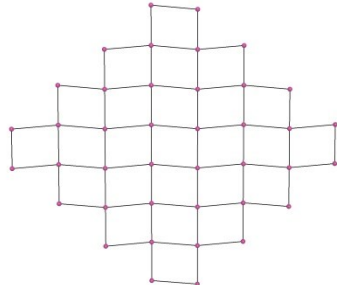
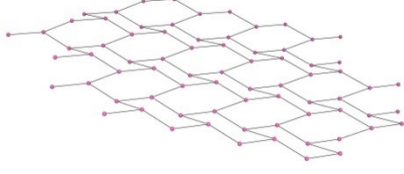
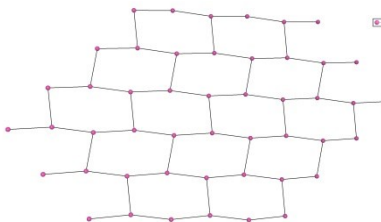
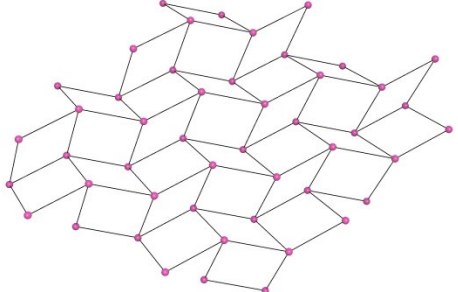
21. S. R. Marshall, C. D. Incarvito, J.L. Manson, A. L. Rheingold, J. S. Miller, *Inorg. Chem.* 2000, 39, 1969-1973.
22. J. Luo, L. Qiu, B. Liu, X. Zhang, F. Yang, L. Cui, *Chin. J. Chem.*, 2012, 30, 522–528.
23. H. Pei, S. Lu, J. Li, Y. Sun, X. Wu, W. Du, *Cryst. Res. Technol.*, 2006, 41, 423–426.
24. W. Huang, J. Zhang, C. Zhang *Acta Cryst.*, 2013, E69, m90.
25. W.-Z. Shen, X.-Y. Chen, P. Cheng, D.-Z. Liao, S.-P. Yan, Z.-H. Jiang, Z. *Anorg. Allg. Chem.*, 2003, 629, 2591–2595.
26. L.-L. Zheng, X.-M. Zhuang, Z. *Anorg. Allg. Chem.*, 2010, 636, 2500–2507.

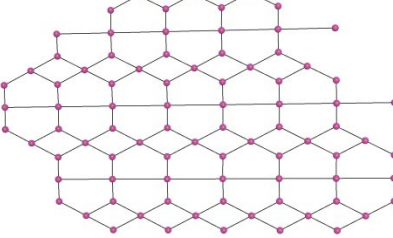
Table S7. Magneto-structural relationships of 2D cobalt(II)-dicyanamido complexes.

Compound/	topology	Co–N _L /Co–O	Co–N _{dca}	Co···Co	Magnetic properties	Ref.
single $\mu_{1,5}$-dca						
[Co(bzim) ₂ (dca) ₂] _n		2.1492(16) 2.1492(16)	2.1152(17) 2.1152(17) 2.1427(18) 2.1427(18)	7.623	$\Theta = 17.14 \text{ K}$ $C = 3.17 \text{ cm}^3 \text{K mol}^{-1}$	27
[Co(pte) ₂ (dca) ₂] _n		2.169(2) 2.169(2)	2.097(2) 2.097(2) 2.146(2) 2.146(2)	8.5739	$C = 3.13 \text{ cm}^3 \text{K mol}^{-1}$ $\Theta = -9.1 \text{ K}$ weak antiferromagnetic interaction	28
[Co ₂ (4-cypy) ₄ (dca) ₄] _n		Co(1) 2.179(7) 2.156(6) Co(2) 2.149(6) 2.181(6)	2.122(6) 2.079(6)	8.037(3) 7.745(3)	J=−1.14K	30

						
[Co(dmdpy)(dca) ₂]		2.142(2) 2.142(2)	2.114(2) 2.095(3) 2.114(2) 2.095(3)	8.102(4)	weak magnetic interaction	32
{[Co(ambzim) ₂ (dca) ₄]} _n		2.1171(13) 2.1171(13)	2.1520(13) 2.1520(13) 2.1591(15) 2.1591(15)	8.186 Å	-	33
{[Co(L ⁶) ₂ (dca) ₂] ₂ (L ⁶)} _n		Co-Owoda= 2.057(5) Co-Owoda= 2.057(5)	2.124(7) 2.124(7) 2.124(6) 2.124(6)	7.894(1)	-	34
[Co(4NOpy) ₂ (dca) ₂ (CH ₃ CN)] _n		2.149, 2.162	2.106, 2.107, 2.110, 2.112	8.13, 8.16	J= -0.8 weak signals for both χ_{mol}' and χ_{mol}	35

[Co(atz) ₂ (dca) ₂] _n		2.1677(15) 2.1677(15)	2.0887(17) 2.0968(16) 2.0887(17) 2.0968(16)	8.041	$\tau_0 = 1.7 \cdot 10^{-6}$ s $E_a = 5.1 \text{ cm}^{-1}$ SIM	38
[Co(bim) ₂ (dca) ₂] _n		2.128(3) 2.134(3)	2.190(3) 2.220(3) 2.209(3) 2.219(3)	8.927(2) 8.968(2)	$ D = 74.3 \text{ cm}^{-1}$ $\tau_0 = 1.54 \cdot 10^{-6}$ s $E_a = 5.33 \text{ cm}^{-1}$ SIM	39
[Co(bmim) ₂ (dca) ₂] _n		2.156(3) 2.163(3)	2.127(3) 2.153(3) 2.152(3) 2.145(3)	8.7110(5) 8.7158(5)	$ D = 75.8 \text{ cm}^{-1}$ $\tau_0 = 0.63 \times 10^{-6}$ s $E_a = 13.81 \text{ cm}^{-1}$ SIM	39
[Co(mepyz) ₂ (dca) ₂]H ₂ O		2.1553(12) 2.1553(12)	2.1210(12) 2.1008(12) 2.1210(12) 2.1008(12)	8.318(6)	$\mu_{\text{eff}} 4.95 \mu_B$	40

(Ph ₄ As)[Co(dca) ₃]		-	2.121 2.121 2.110 2.110 2.140 2.140	7.370 8.650	no long-range magnetic interaction	31
[Co(phen)(dca) ₂] _n		2.1344(14) 2.1209(13)	2.1346(16) 2.1085(14) 2.2109(16) 2.0845(15)	7.2571(3) 7.6017(3)	J= -0.33 cm ⁻¹ Θ = -0.017K	46
[Co(2,9-dmphen)(dca) ₂] _n		2.1707(15) 2.1884(16)	2.1491(17) 2.1097(18) 2.0871(18) 2.1269(18)	7.389(1) 7.718(1)	J= -0.03 cm ⁻¹ Θ = -0.005K	46
[Co(dca) ₂ (pypz)] _n		2.166(2) 2.130(3)	2.130(2) 2.123(3) 2.107(3) 2.093(3)	8.899 Å	-	16

double $\mu_{1,5}$-dca + double $\mu_{1,3,5}$-dca					
[Co(dca) ₂ (H ₂ O)]·phz		Co(2)-Owoda = 2.049(2)	Co(1)	7.4110	$\mu_{\text{Co}} = 4.84 \mu_B$
		2.080(2)		9.7995	36
		2.086(2)			
		Co(2)-Owoda = 2.049(2)	2.213(2)		
		2.080(2)			
		2.086(2)			
		2.213(2)			
		Co(2)			
		2.121(2)			
		2.163(2)			
		2.121(2)			
		2.163(2)			
$\mu_{1,5}$-dca + $\mu_{1,3,5}$-dca					
[Co(pzdo)(dca) ₂]	-	Co-O=2.124(4)	Co(1)	7.499 Å	$\Theta = -9.4 \text{ K}$
		2.100(3)			$C = 3.17 \text{ cm}^3 \text{ mol}^{-1} \text{ K}$
		Co-O=2.124(4)	2.100(3)		
		2.100(3)			
		Co(2)			
		2.179(4)			
		2.179(4)			
[Co ₂ (modo) ₂ (dca) ₄]	-	Co-O=2.122(2)	2.065(2)	5.803,	$C = 6.61 \text{ cm}^3 \text{ mol}^{-1}$
		2.065(2)		7.877	K
		Co-O=2.122(2)	2.178(2)		$\Theta = -33.5 \text{ K}$
		2.089(2)			
[Co(pydz) ₂ (dca) ₂] _n	-	2.140(3)	2.122(2)	7.3474(2)	$C = 3.50 \text{ cm}^3 \text{ K mol}^{-1}$
		2.088(2)		6.0490(6)	
		2.122(2)			$\Theta = -18.11 \text{ K}$
		2.088(2)			$\mu_{\text{eff}} = 5.29 \mu_B$
		2.231(3)			
		2.231(3)			

double $\mu_{1,5}$ -dca + ligand						
[Co(bnzd)(dca) ₂] _n		2.1895(16) 2.1895(16)	2.1173(16) 2.1173(16)	7.293 through dca 12.941 through bnzd	J = -3.38 K weak antiferromagnetic interaction	29
{[Co(L ⁷) ₂ (dca)](OH)(gly) ₂ } _n		2.182 2.163	2.140 2.140 2.163 2.163	8.8 through dca 14.5 through ligand	-	37
[Co(3bpo)(dca) ₂] _n		2.176(4) 2.160(4)	2.091(4) 2.103(5) 2.136(4) 2.115(4)	7.383(6)	it is impossible to fit the magnetic data of 2-D Co ^{II}	41
[Co(btm) ₂ (dca)]ClO ₄		2.146(5) 2.140(5) 2.151(5) 2.143(5) Co(2) 2.156(6) 2.156(6) 2.136(6) 2.136(6)	2.084(5) 2.072(5)	8.539(2) 8.910(3)	weak antiferromagnetic interaction	42

L⁶= pyridinium-4-olate; **L⁷**= bis[3,5-dimethyl-4-(49-pyridyl)pyrazol-1-yl]methane; **bzim** = benzimidazole; **pte** = 1-(2,4-difluorophenyl-2- (1H-1,2,4-triazol-1-yl)ethanone, **bnzd**= benzidine; **4cypy**= 4- cyanopyridine, **dmdpy**= 5,5'-dimethyl-2,2'-dipyridine; **ambzim**= 2-aminobenzimidazole; **4NOp**y= 4-(N-tert-butylamino)pyridine; **pypz**= 3,5-dimethyl-1-(2-pyridyl)pyrazole; **phz**= phenazine; **atz**= 2-amino-

1,3,5-triazine; **bim**=1-benzylimidazole, **bmim**= 1-benzyl-2-methylimidazole; **mepyz**= methylpyrazine; **3bpo**= 2,5-bis(3-pyridyl)-1,3,4-oxadiazole; **btrm**= 1,2-bis(1,2,4-triazole-1-yl)methane; **pzdo**= pyrazine dioxide; **modo**= 2,3,5-trimethylpyrazine-dioxide; **phen**= 1,10-phenanthroline; **2,9-dmphen**= 2,9-dimethylphenanthroline

27. S. Wang, L. Wang, B. Li, Y. Zhang, *J. Chem. Crystallogr.*, 2009, **39**, 221–224.
28. L. Zhang, Y. Ling, A.-X. Hu, T.-T. Yao, J. Li, *Inorg. Chim. Acta*, 2009, **362**, 4867–4874.
29. S. Khan, S. Roy, K. Bhar, R. Ghosh, C.-H. Lin, J. Ribas, B. Kumar Ghosh, *Inorg. Chim. Acta*, 2013, **398**, 40–45
30. M. Du, Q. Wang, Y. Wang, X.-J. Zhao, J. Ribas, *J. Solid State Chem.*, 2006, **179**, 3926–3936
31. P. M. van der Werff, S. R. Batten, P. Jensen, B. Moubaraki, K. S. Murray, E. H.-K. Tan, *Polyhedron*, 2001, **20**, 1129–1138
32. L. B. Lopes, C.C. Corrêa, G.P. Guedes, M.G.F. Vaz, R. Diniz, F. C. Machado, *Polyhedron*, 2013, **50**, 16–21
33. A. Das, B. Bhattacharya, D. Kumar Maity, A. Halder, D. Ghoshal, *Polyhedron*, 2016, **117**, 585–591.
34. L. Zheng, *Journal of Chemistry*, 2013, 1-10.
35. H. Ogawa, K. Mori, K. Murashima, S. Karasawa, N. Koga, *Inorg. Chem.* 2016, **55**, 717–728.
36. A. M. Kutasi, S. R. Batten, B. Moubaraki, K. S. Murray, *J. Chem. Soc., Dalton Trans.*, 2002, 819–821.
37. M. Du, X.-G. Wang, Z.-H. Zhang, L.-F. Tang, X.-J. Zhao, *CrystEngComm*, 2006, **8**, 788–793.
38. J. Palion-Gazda, T. Klemens, B. Machura, J. Vallejo, F. Lloret, M. Julve, *Dalton Trans.*, 2015, **44**, 2989–2992.
39. A. Świtlicka-Olszewska, J. Palion-Gazda, T. Klemens, B. Machura, J. Vallejo, J. Cano, F. Lloret, M. Julve, *Dalton Trans.*, 2016, **45**, 10181–10193.
40. A. M. Kutasi, A. R. Harris, S.R. Batten, B. Moubaraki, K. S. Murray, *CrystGrowth&Des.*, 2004, **4**, 605-610.
41. M. Du, Q. Wang, C.P. Li, X.-J. Zhao, J. Ribas, *CrystGrowth&Des.*, 2010, **10**, 3285– 3296.
42. X.-Y. Chen, P. Cheng, S.-P. Yan, D.-Z. Liao, Z.-H. Jiang, Z. *Anorg. Allg. Chem.* 2005, **631**, 3104–3107
43. H.-L. Sun, S. Gao, B.-Q. Ma, G. Su, *Inorg. Chem.*, 2003, **42**, 53995404.
44. H.-L. Sun, Z.-M. Wang, S. Gao, *Inorg. Chem.*, 2005, **44**, 2169–2176

3. The HFEPR and FIRMS spectra

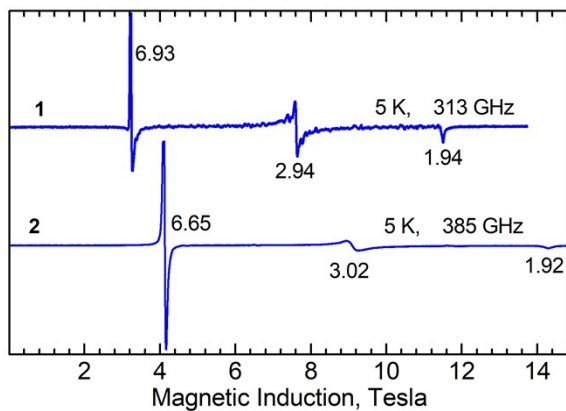


Figure S8. Blue traces: HF EPR spectra of compounds **1** and **2** recorded at similar conditions.

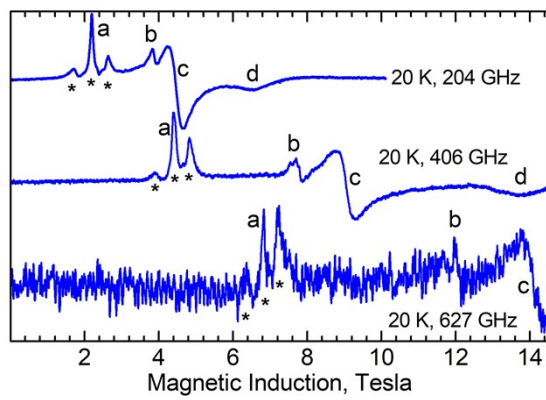


Figure S9. Blue traces: HF EPR spectra of compound **3**.

4. Selected AC susceptibility data

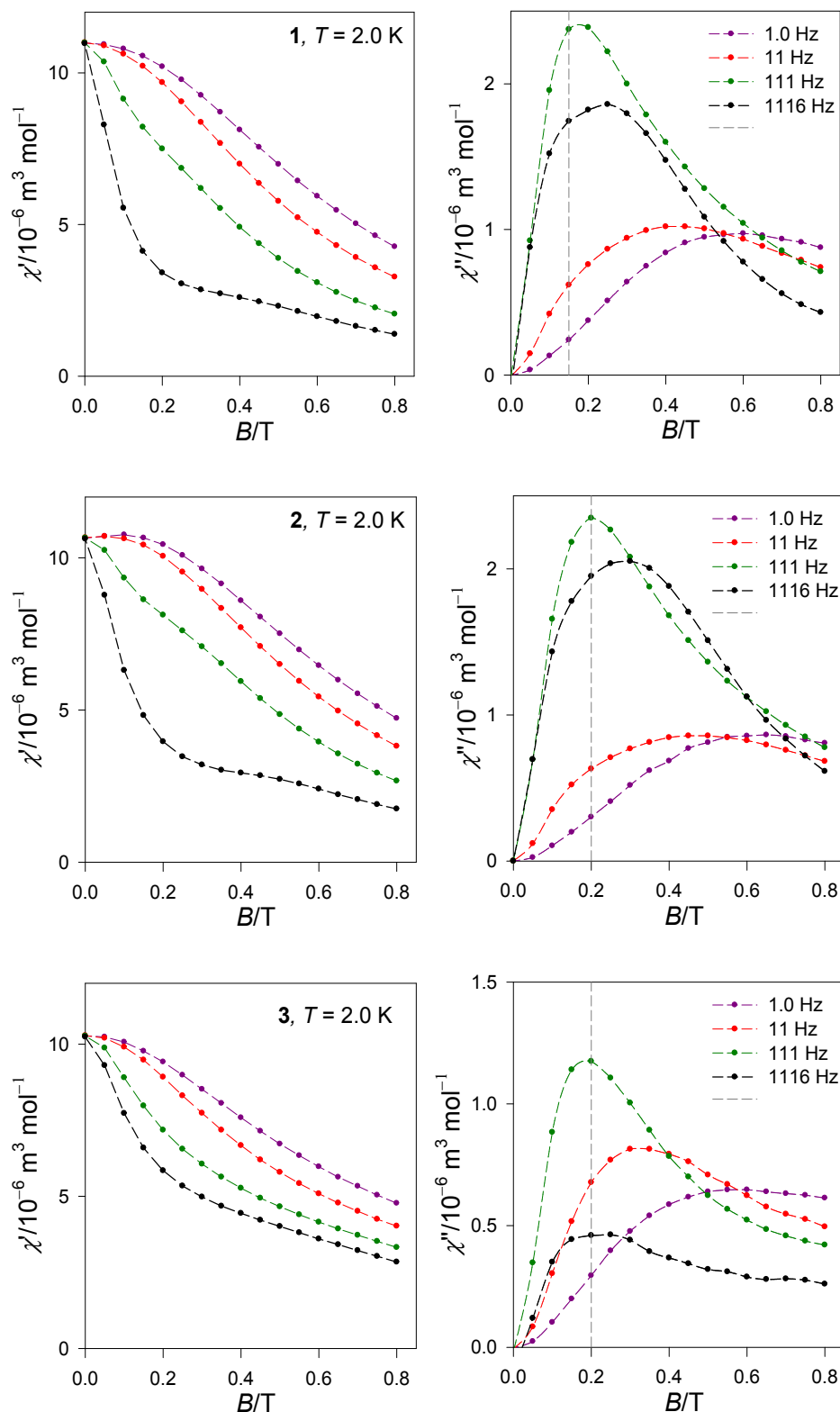


Figure S10. Field dependence of the AC susceptibility for **1** through **3** at $T = 2.0\text{ K}$ for a set of trial frequencies. Lines – guide for eyes.

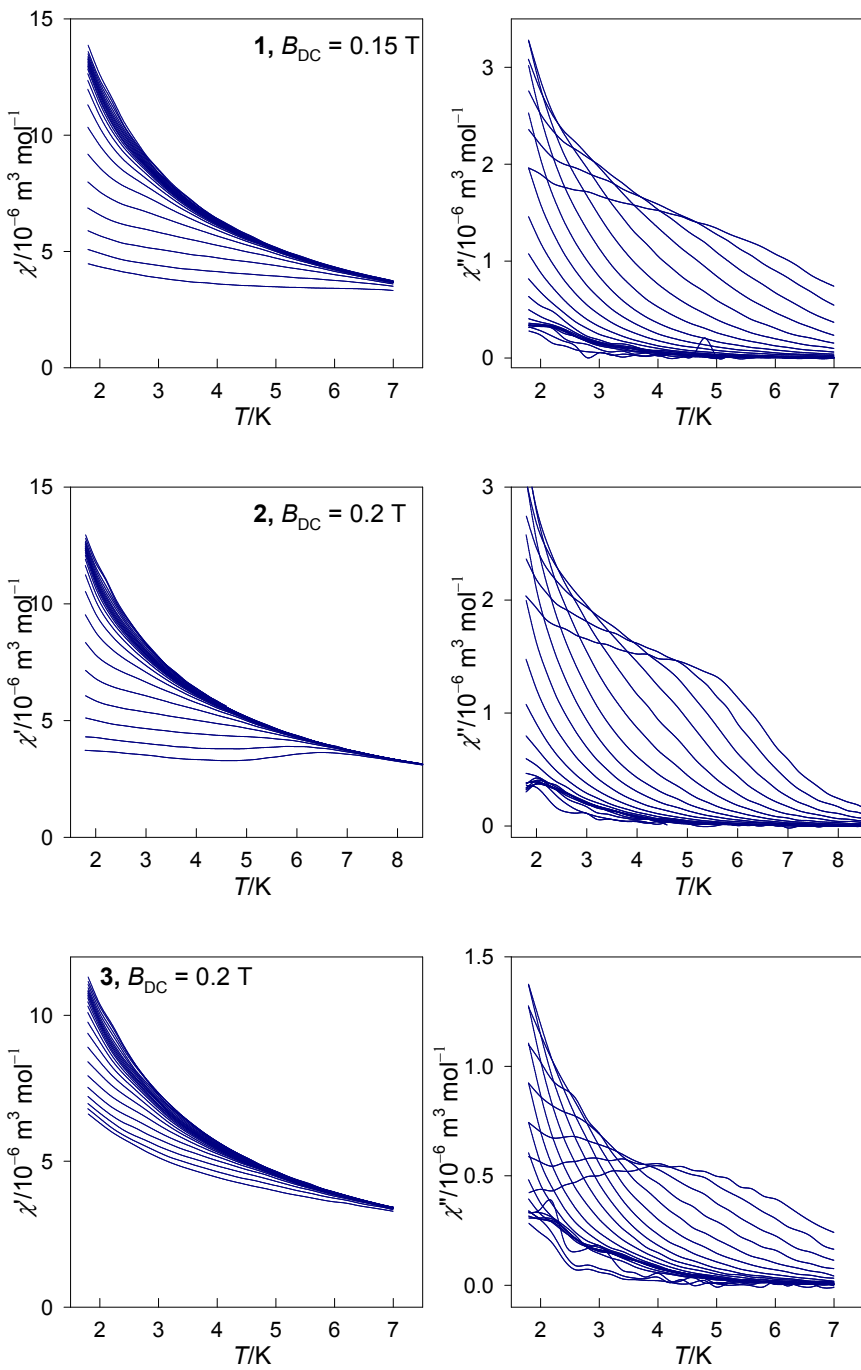


Figure S11. Temperature dependence of the AC susceptibility for **1** through **3** at $B_{DC} = 0.2 \text{ T}$ for 22 frequencies of the oscillating field.

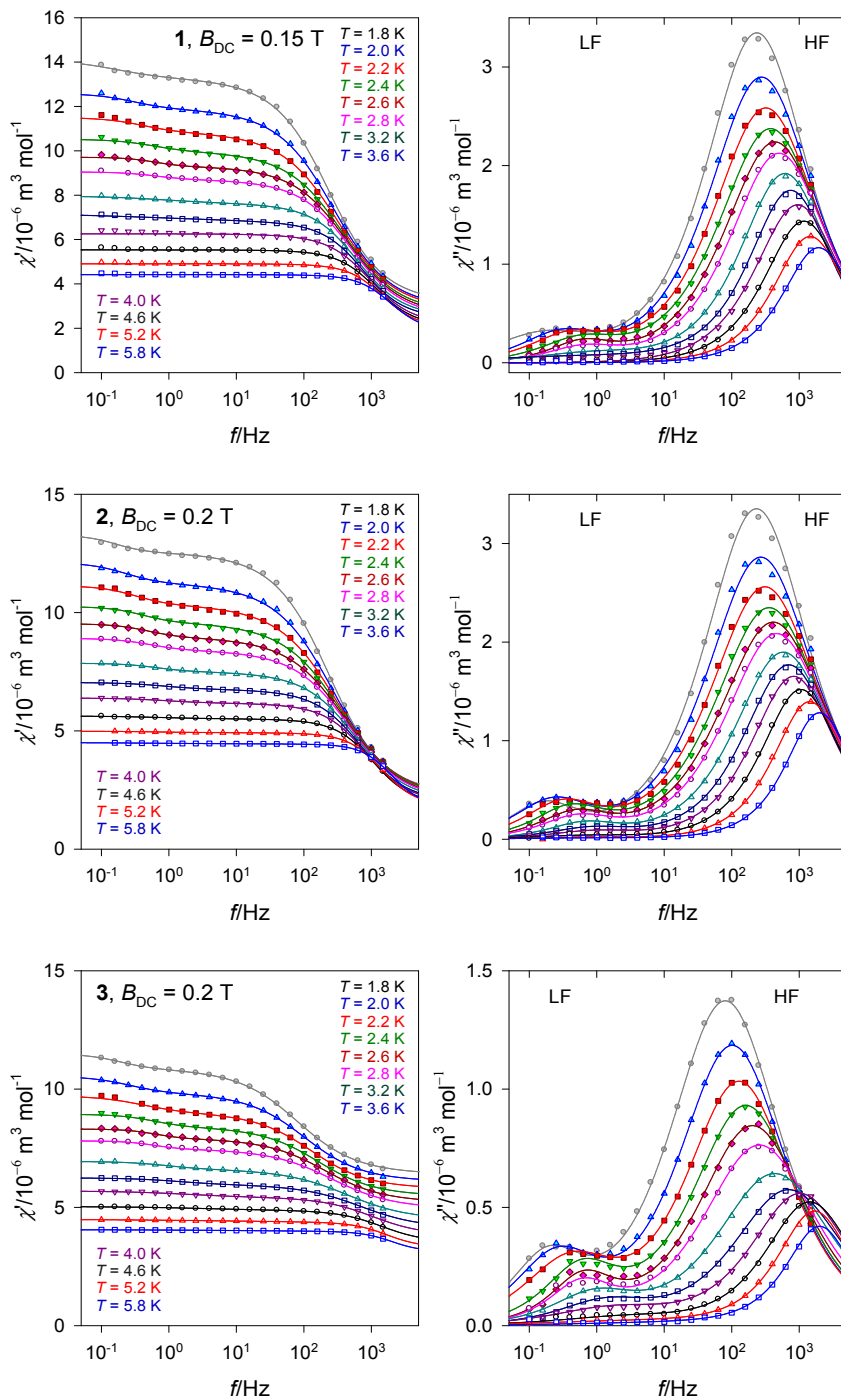


Figure S12. Frequency dependence of the AC susceptibility at $B_{DC} = 0.2$ T. Lines – fitted, using the two-set Debye model.

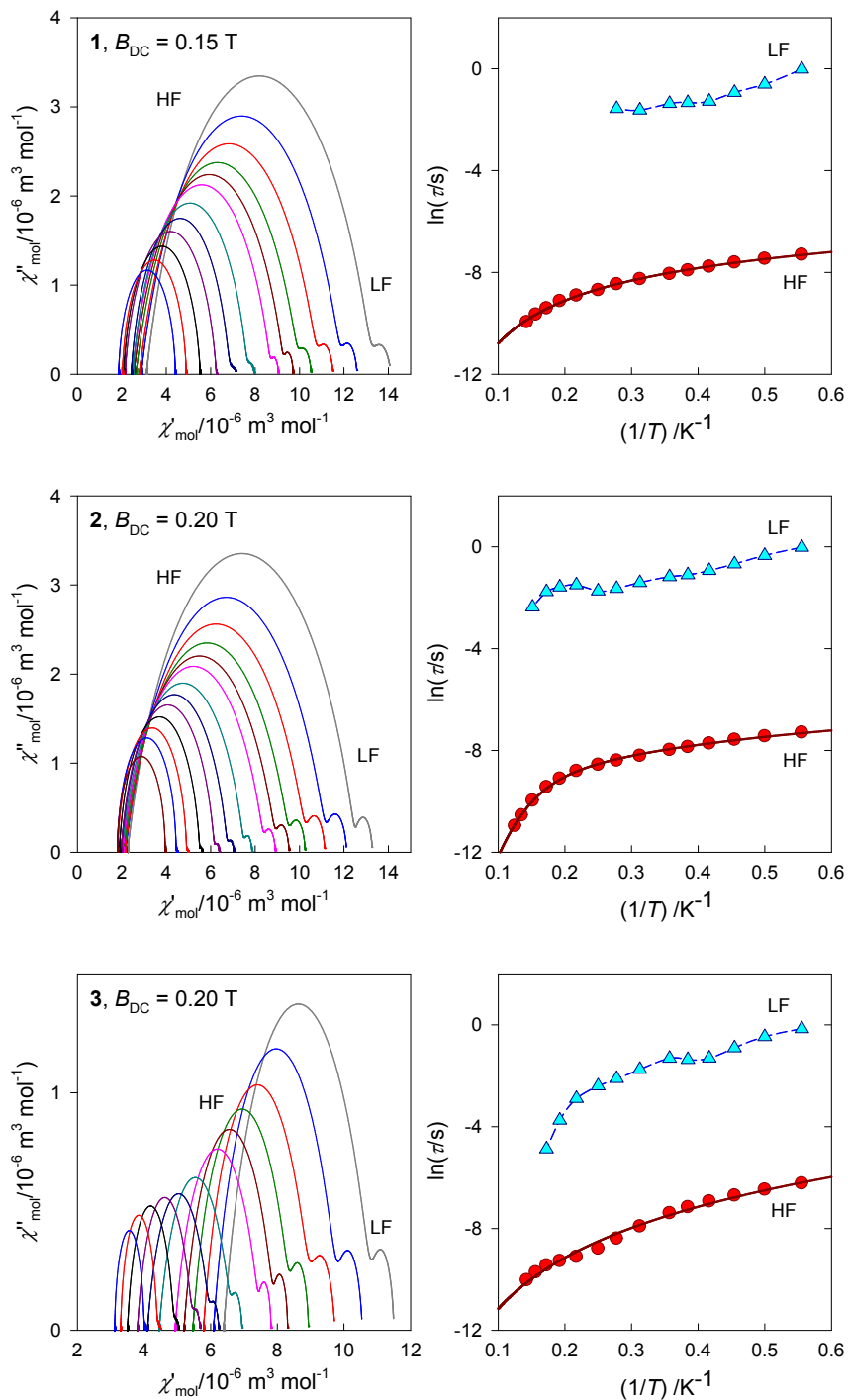


Figure S13. Argand plot (left) and the Arrhenius-like plot (right). Solid line – fitted with Raman-like and phonon-bottleneck terms $\tau^{-1} = CT^n + FT^l$.

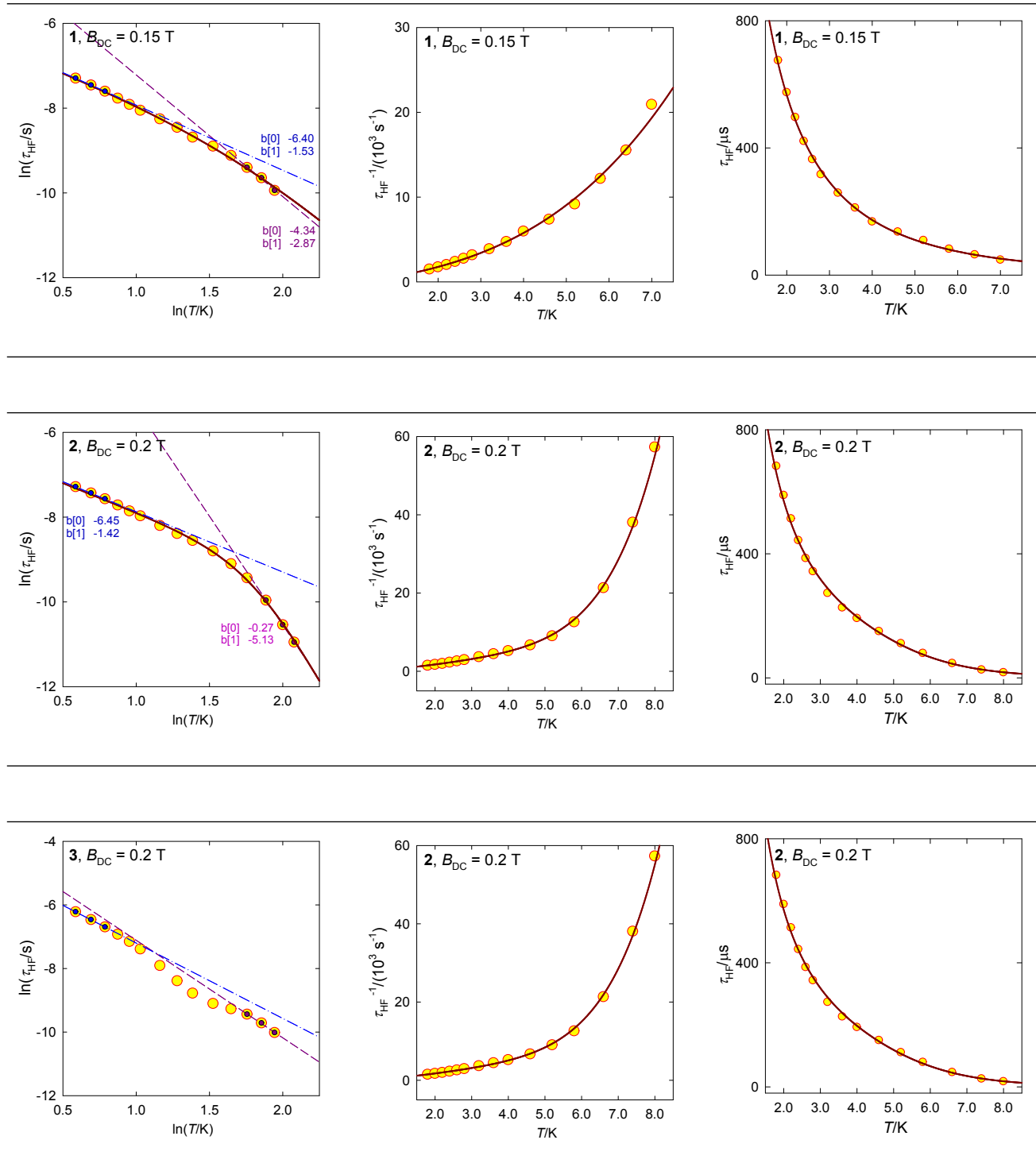


Figure S14. Various dependences of the high-frequency relaxation time. Dashed (dot-dashed) lines – linear fits to the high-temperature (low-temperature) windows. Solid – combined Raman-like and phonon-bottleneck terms.